Materials Science & Engineering A 610 (2014) 17–27

Contents lists available at ScienceDirect

Materials Science & Engineering A

journal homepage: www.elsevier.com/locate/msea

Softening by severe plastic deformation and hardening by annealing of aluminum–zinc alloy: Significance of elemental and spinodal decompositions

Ali Alhamidi [a,b,*], Kaveh Edalati [a,b], Zenji Horita [a,b], Shoichi Hirosawa [c], Kenji Matsuda [d], Daisuke Terada [e]

[a] Department of Materials Science and Engineering, Faculty of Engineering, Kyushu University, Fukuoka 819-0395, Japan
[b] WPI, International Institute for Carbon-Neutral Energy Research (WPI-I2CNER), Kyushu University, Fukuoka 819-0395, Japan
[c] Department of Mechanical Engineering and Materials Science, Yokohama National University, Yokohama 240-8501, Japan
[d] Graduate School of Science and Engineering for Research, University of Toyama, Toyama 930-8555, Japan
[e] Department Materials Science and Engineering, Faculty of Engineering, Kyoto University, Kyoto 606-8501, Japan

ARTICLE INFO

Article history:
Received 29 April 2014
Accepted 9 May 2014
Available online 20 May 2014

Keywords:
Severe plastic deformation (SPD)
High-pressure torsion (HPT)
Ultrafine-grained (UFG) materials
Phase transformation
Solution hardening

ABSTRACT

An Al–30 mol% Zn supersaturated solid solution alloy was severely deformed using high-pressure torsion (HPT) at 300 K and subsequently annealed at 373–673 K. The hardness and tensile strength significantly decreased and the tensile ductility increased with straining by HPT and reached a steady-state level at large imposed strains. Despite this softening behavior, the lattice strain was increased, Zn-rich particles were precipitated and the initial coarse grains were refined significantly to a size of ~190 nm while being accompanied by decomposition to Al- and Zn-rich phases because of rapid atomic diffusion. The subsequent annealing led to a hardening, but microstructural observations showed that decrease in the lattice strain, increase in the grain size and reduction in the fraction of precipitates occurred by annealing. It was shown that the unusual softening/hardening behavior of the Al–Zn alloy was mainly due to the contribution of spinodal decomposition. The formation of nano-sized lamellae by spinodal decomposition resulted in increase in hardness after solution treatment and after post-HPT annealing, while this lamellar structure was destroyed by HPT, which resulted in softening. The softening was less significant when the hardness was evaluated at low homologous temperatures.

1. Introduction

Severe plastic deformation (SPD) methods such as Equal-Channel Angular Pressing (ECAP) [1–6], Accumulative Roll-Bending (ARB) [7,8] and High-Pressure Torsion (HPT) [9–18] are well-known processing procedures in which high densities of lattice defects and ultrafine grains (UFG) are achieved in metallic materials by imparting large strains. Among the different techniques for the SPD process introduced so far (see reviews in Refs. [18–21]), HPT is especially effective to introduce large plastic strains for grain refinement up to a steady state [9–18] where the hardness and microstructure remain unchanged with straining. The method is also capable of controlling the solid-state phase transformations in metallic materials [22–25] and even in non-metallic materials such as Si [26], C [27] and ZrO_2 [28].

In general, most metallic materials show hardening due to grain refinement through the Hall–Petch relationship. However, recent papers reported three different types of hardness–strain behaviors after HPT processing. First, in metals with high melting temperatures such as Fe and Ti, a steady state is reached directly following the initial hardening with straining [10,11,13,29]. Second, in metals with moderate melting temperatures such as Al and Mg, the hardness initially increases with increasing strain and, after reaching a maximum, decreases to a steady-state level [30–34]. This behavior was also detected in several metals and alloys when processed at high homologous temperatures [29,35–37]. Third, in metals with low melting temperatures such as Zn, Pb, Sn and In, the hardness slightly decreases with an increase in strain at an early stage of straining and enters into a steady state at large strains [29,38]. This strain softening behavior was also reported in nanograined Ni [12,13] as well as in several alloys such as a Pb–Sn eutectic alloy [39], a Zn–Al–Cu alloy [40], Zn–Al monotectoid alloys [39–42] and Al–Zn alloys [43–51].

* Corresponding author at: Department of Materials Science and Engineering, Faculty of Engineering, Kyushu University, Fukuoka 819-0395, Japan.
Tel./fax: +81 92 802 2992.
E-mail addresses: ali@zaiko6.zaiko.kyushu-u.ac.jp, aldi.hamidi@gmail.com (A. Alhamidi).

http://dx.doi.org/10.1016/j.msea.2014.05.026
0921-5093/

Although several publications reported a significant decrease in hardness up to 130 Hv in the Al–Zn alloys after SPD processing using the HPT method [43–51], the mechanism for this unusual softening is not clearly understood. softening in the Al-Zn alloy, which was also reported during cold rolling [52], ball milling [53] and ECAP [54,55], was mainly attributed to elemental decomposition and reduction of solid solution hardening. However, as shown in Appendix 1, the theoretical models such as the Fleischer model [56] and the Labusch model [57] predict a small solid solution hardening in the Al–Zn alloys because of weak elastic and modulus interactions between solute atoms and matrix.

In this study, we thus investigate the softening mechanism in an Al–30 mol% Zn (~51 wt% Zn) alloy by HPT and show the critical importance of spinodal decomposition and homologous temperature on this softening. The evolutions of microstructure and mechanical properties along with HPT processing as well as after subsequent annealing are investigated.

2. Experimental procedures

Pure Al (99.99%) was alloyed with 30 mol% Zn (99.99%) by melting in air at 1123 K in an alumina crucible. According to the Al–Zn phase diagram, the alloy exhibits a liquidus temperature (Liq.→α+Liq.) at 830 K, solidus temperature (α+Liq.→α) at 750 K, phase separation at 610 K ($\alpha \rightarrow \alpha_1 + \alpha_2$) and monotectoid transformation ($\alpha_2 \rightarrow \alpha_1 + \beta$) at 550 K (α: Al–Zn solid solution with the fcc structure, α_1, α_2: Al-rich and Zn-rich phases with the fcc structure, respectively, β: Zn-rich phase with the hcp structure) [58]. The alloy was cast into a mold with dimensions of $30 \times 20 \times 80$ mm^3. The ingot was homogenized at 703 K for 24 h and cooled in air. The homogenized ingot was sliced into sheets with 8 mm thickness using a wire-cutting electrical discharge machine. The sheets with 8 mm thickness were rolled at room temperature and their thickness was reduced to 1.2 mm.

The cold-rolled sheets were subsequently solution-treated at 673 K for 1 h and quenched rapidly in ice water to give an initial grain size of ~130 μm (as in Fig. 1(a)) with a hardness of 182 Hv. It should be noted that this hardness is unusually high because a spinodal decomposition occurred during the rapid cooling as will be mentioned later. The sheets after the solution treatment (hereafter, called S.T.) were cut to discs with 10 mm diameter and 1.2 mm thickness and HPT was carried out on the discs at room temperature (~300 K) under a pressure of $P=6$ GPa for $N=1$, 3, 10 and 25 revolutions using the facilities described in details earlier [11,59]. The HPT-processed samples after $N=25$ revolutions were annealed at 373, 423, 473, 523, 593, 623, 643 and 673 K for 24 h and cooled down rapidly in air. Annealing was also conducted on the HPT-processed samples after $N=25$ revolutions at 373 K for different periods of time such as 0.5, 1, 5 and 24 h. All samples were kept in a freezer at a temperature of 243 K before processing as well as before experimental analyses.

As reference materials, discs of pure Al (99.99%) and Zn (99.99) with 10 mm diameter and 0.8 mm thickness were also used in this study. The discs of Al and Zn were annealed for 1 h at 773 K and 523 K, respectively, under an argon atmosphere to give a grain size of ~1 mm for Al and ~390 μm for Zn. HPT was carried out on the annealed discs at room temperature under a pressure of $P=6$ GPa for $N=5$ and 15 revolutions.

Following the HPT processing and annealing, the Vickers microhardness was measured at 300 K with an applied load of 200 g for 15 s along 12 radial directions of the discs with an incremental step of 0.5 mm. The Vickers microhardness measurements were also carried out on several samples at cryogenic temperatures (~90 K) in liquid nitrogen.

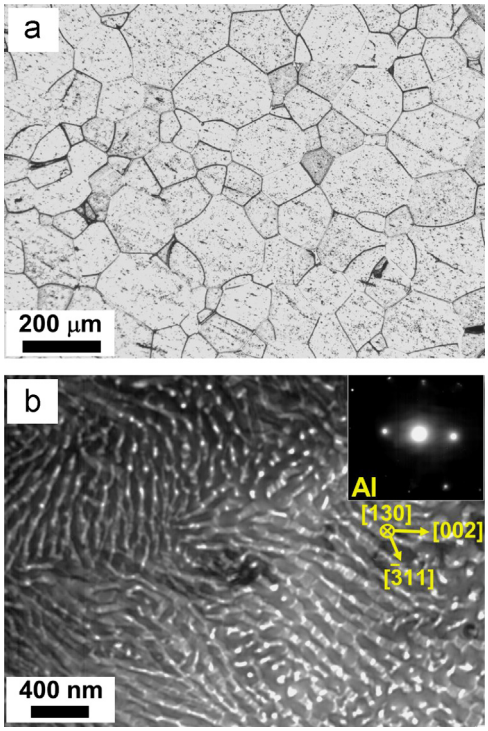

Fig. 1. (a) Optical micrograph and (b) TEM bright-field image and the corresponding SAED pattern of sample after cold rolling and solution treatment at 673 K for 1 h.

Crystallographic structures were analyzed by X-ray diffraction (XRD) analysis using the Cu Kα radiation in a scanning step of 0.01–0.02° and a scanning speed of 0.5–1°/min. The XRD patterns were obtained from a ~3 mm diameter region at the edge of the discs. LaB_6 standard powders were used concurrently with the samples during XRD analysis for offsetting any possible peak shifts between measurements.

For transmission electron microscopy (TEM) and scanning transmission electron microscopy (STEM), thin samples were prepared at 3.5 mm away from the center of the HPT-processed discs using either a focused ion beam system or a twin-jet electrochemical polisher in a solution of 33% HNO_3 and 67% CH_3OOH at 263 K under a voltage of 18 V. TEM and STEM were performed at 200 and 300 kV, respectively, for microstructure observation, selected-area electron diffraction (SAED) analysis and energy dispersive X-ray spectrometry (EDS).

For examination of tensile properties, miniature tensile specimens having gauge dimensions of 1.5 mm length, 0.5–0.7 mm width and 0.5 mm thickness were cut from the discs at the position 2 mm away from the disc center using a wire-cutting electrical discharge machine. Each tensile specimen was mounted horizontally on grips and pulled to failure using a tensile testing machine with an initial strain rate of 2×10^{-3} s^{-1}.

3. Results

Fig. 1(b) shows a TEM bright-field image and the corresponding SAED pattern of a sample after solution treatment. It is apparent that the initial coarse microstructure consists of very fine lamellae with a width of ~35 nm. The SAED pattern corresponds to the α phase with the fcc structure, confirming that the structure consists of a single grain and a single crystallographic structure. Since no evidence for the Zn-rich β phase was found using SAED and XRD analysis (see Fig. 4 for XRD profiles of solution-treated